of the observed structure prepared under a number of conditions illustrates that the Cu layers between the Ba layers are those most easily affected. There has been a report, based upon the surface-sensitive technique of X-ray photoelectron spectroscopy (XPS),[8] that oxygen could be extracted from the Ba layers by preparing the material under vacuum, rather than under a reducing atmosphere, such as nitrogen or argon. We found no evidence for this in the material we prepared under vacuum. The crystal structure of this material contained oxygen vacancies only in the Cu layers between the Ba layers. Any Ba layer vacancy observed by XPS, is, therefore, a surface rather than a bulk phenomenon.

High-temperature neutron diffraction,[9] which is much more sensitive to oxygen than is X-ray diffraction, suggests that the high-temperature tetragonal form actually has oxygen in these Cu layers, but since the positions are now symmetry related, the population is uniformly distributed among the four positions. Our attempts at trying to prepare a quenched sample where the oxygen might be trapped in this layer were not successful. The powder pattern of this sample showed it to be a mixture of the tetragonal and orthorhombic forms. A tetragonal crystal was found (although the quality was not as good as the other preparations), and the structure was determined. Although there appeared to be some electron density in the oxygen positions of the Cu layers, the refinement of the occupancy of the site yielded standard deviations as large as the occupancy and large thermal parameters. We, thus, cannot conclusively identify any occupancy by oxygen in the tetragonal material we have examined. The existence of additional oxygen in the tetragonal material that first forms a high-temperature in air or oxygen, however, is supported by TGA analysis.[10] There is less weight loss at 700 °C in air or oxygen than there is in nitrogen, presumably due to more oxygen in the structure.

This exercise does illustrate, however, that it is very easy to obtain the orthorhombic material in a quenching experiment. Presumably, since the oxygen uptake is diffusion controlled, a thin layer of the oxygen-rich orthorhombic material may form in any sample that is quenched in air or oxygen. Reports of some superconductivity in tetragonal material[11] may be related to a small amount of the orthorhombic material on the surface of the tetragonal particles.

The facile transformation between the orthorhombic and tetragonal forms of this material illustrates both the rigidity of the perovskite framework and the mobility of oxygen in this system. Atmosphere and temperature are, therefore, important parameters to control in the fabrication of any devices containing this material. The oxygen-starved structure of the tegragonal form of the material could provide an interesting starting point for the introduction of other elements (e.g. F) into this framework.

Acknowledgment. We thank J. F. Ackerman for the vacuum preparation of this material, N. A. Marotta for the TGA measurements, and W. G. Morris for helpful discussions regarding this work.

Registry No. $Ba_2YCu_3O_6$, 109489-85-2.

Supplementary Material Available: Table SI of anisotropic thermal parameters for the 700 °C nitrogen preparation structure (1 page); tables of observed and calculated structure factors for each of the five structures (3 pages). Ordering information is given on any current masthead page.

(8) Schrott, A. G.; Park, S. I.; Tsuei, C. C., to be submitted for publication.
(9) Jorgensen, J. D.; Beno, M. A.; Hinks, D. G.; Soderholm, K. J.; Volin, K. J.; Hitterman, R. L.; Grace, J. D.; Schuller, I. K.; Segre, C. U.; Zhang, K.; Kleefisch, M. S., submitted for publication in *Phys. Rev.*
(10) Gallagher, P. K.; O'Bryan, H. M.; Sunshine, S. A.; Murphy, D. W. *Mater. Res. Bull.* **1987**, *22*, 995.
(11) Kini, A. M.; Geiser, U.; Kao, H.-C. I.; Carlson, K. D.; Wang, H. H.; Monaghan, M. R.; Williams, J. M. *Inorg. Chem.* **1987**, *26*, 1834.

Contribution from the Institut de Chimie Minérale et Analytique, University of Lausanne, 3, Place du Château, CH-1005 Lausanne, Switzerland, and Institut für Anorganische Chemie, University of Bern, CH-3000 Bern 9, Switzerland

Variable-Temperature and Variable-Pressure NMR Kinetic Study of Solvent Exchange on $Ru(H_2O)_6^{3+}$, $Ru(H_2O)_6^{2+}$, and $Ru(CH_3CN)_6^{2+}$ [1,2]

Irina Rapaport,[3a] Lothar Helm,[3a] André E. Merbach,*[3a] Paul Bernhard,[3a,b] and Andreas Ludi*[3b]

Received August 26, 1987

Water exchange on ruthenium(II) and ruthenium(III) was studied by ^{17}O NMR and acetonitrile exchange on ruthenium(II) was studied by ^1H NMR spectroscopy as a function of temperature and pressure. For ruthenium(II), the kinetic parameters are as follows: (a) $Ru(H_2O)_6^{2+}$, $k^{298} = (1.8 \pm 0.2) \times 10^{-2}$ s^{-1}, $\Delta H^{\ddagger} = 87.8 \pm 4$ kJ mol^{-1}, $\Delta S^{\ddagger} = +16.1 \pm 15$ J K^{-1} mol^{-1}, $\Delta V^{\ddagger} = -0.4 \pm 0.7$ cm^3 mol^{-1}; (b) $Ru(CH_3CN)_6^{2+}$, $k^{298} = (8.9 \pm 2) \times 10^{-11}$ s^{-1}, $\Delta H^{\ddagger} = 140.3 \pm 2$ kJ mol^{-1}, $\Delta S^{\ddagger} = +33.3 \pm 6$ J K^{-1} mol^{-1}, $\Delta V^{\ddagger} = +0.4 \pm 0.6$ cm^3 mol^{-1}. This implies that the solvent exchange on Ru^{2+} occurs via an interchange I mechanism for both H_2O and CH_3CN. For ruthenium(III) in water the observed rate constant was of the form $k = k_1 + k_2/[H^+]$ where subscripts 1 and 2 refer to the exchange pathways on $Ru(H_2O)_6^{3+}$ and $Ru(H_2O)_5OH^{2+}$, respectively; the kinetic parameters are as follows: $k_1^{298} = (3.5 \pm 0.3) \times 10^{-6}$ s^{-1}, $\Delta H_1^{\ddagger} = 89.8 \pm 4$ kJ mol^{-1}, $\Delta S_1^{\ddagger} = -48.3 \pm 14$ J K^{-1} mol^{-1}, $\Delta V_1^{\ddagger} = -8.3 \pm 2.1$ cm^3 mol^{-1}; $k_2^{298} = (1.1 \pm 0.2) \times 10^{-6}$ *m* s^{-1}, $\Delta H_2^{\ddagger} = 136.9 \pm 6$ kJ mol^{-1}, $\Delta S_2^{\ddagger} = +100.5 \pm 18$ J K^{-1} mol^{-1}, $\Delta V_2^{\ddagger} = -2.1 \pm 1.4$ cm^3 mol^{-1}. Estimations of the first-order rate constant (using the relation $k_2 = k_{OH}K_{a1}$) and the corresponding activation volume for $Ru(H_2O)_5OH^{2+}$ are $k_{OH}^{298} = 5.9 \times 10^{-4}$ s^{-1} and $\Delta V_{OH}^{\ddagger} = +0.9$ cm^3 mol^{-1}. These data are conclusive for an associative interchange I_a mechanism for water exchange on $Ru(H_2O)_6^{3+}$ but for an I mechanism on the deprotonated species $Ru(H_2O)_5(OH)^{2+}$. These mechanistic results for low-spin ruthenium solvates are compared to those of other di- and trivalent transition-metal ions.

Introduction

A large number of substitution reactions on Ru(II) and Ru(III) have been investigated over the last 25 years. Most studies dealt with complexes in which only one ligand was replaced, the $(NH_3)_5RuX^{2+}$ ions playing a dominant role.[4] Information about the rates of such processes was often obtained from combined electron-transfer and substitution studies, and it was soon realized that substitution on Ru(III) could often be catalyzed by the

(1) High Pressure NMR Kinetics. 34. Part 33: See ref 2.
(2) Cossy, C.; Helm, L.; Merbach, A. E. *Helv. Chim. Acta* **1987**, *70*, 1516.
(3) (a) University of Lausanne. (b) University of Bern.
(4) Endicott, J. F.; Taube, H. *J. Am. Chem. Soc.* **1962**, *84*, 4984. Stritar, J. A.; Taube, H. *Inorg. Chem.* **1969**, *8*, 2281. Taube, H. *Comments Inorg. Chem.* **1981**, *1*, 17 and references therein.

0020-1669/88/1327-0873$01.50/0 © 1988 American Chemical Society

presence of Ru(II) due to rapid electron transfer between the two ions,[5] analogous to the Cr(II)–Cr(III) systems. From these studies it was concluded that Ru(III) complexes tended to react via an associative pathway and Ru(II) predominantly via a dissociative pathway.

The main evidences for an associative mechanism on Ru(III) were (1) a strong dependence of the substitution rate upon the nature of the incoming group in the substitution on Ru(EDTA)H_2O^-,[6] (2) complete stereoretention in the substitution and base hydrolysis of chiral complexes,[7] and (3) large negative volumes of activation in the aquation of $Ru(NH_3)_5Cl^{2+}$ and the anation of $Ru(NH_3)_5H_2O^{3+}$ (−30 and −20 cm^3 mol^{-1}, respectively).[8] Recently it was proposed[9] that the initial step in the oxidation of water by the complexes $M(bpy)_3^{3+}$ (bpy = 2,2′-bipyridine; M = Fe, Ru, Os) is the attack of H_2O at the M(III) center to form a seven-coordinate intermediate.

In the case of Ru(II) it was found that (1) for *cis*-$[Ru(phen)_2(py)_2]^{2+}$ the rate of substitution of py by X^- (Cl^-, Br^-, I^-, NCS^-, N_3^-, NO_2^-) was independent of the nature of X^-[10] and (2) rates and enthalpies of activation for the substitution of H_2O by Cl^-, Br^-, and I^- in the $Ru(H_2O)_6^{2+}$ solvate were very similar,[11] indicating that the activation steps are identical for the different halides (i.e. dissociation of H_2O). The implication of this study[11] was that the water exchange rate for $Ru(H_2O)_6^{2+}$ should be $\sim 10^{-1}$ s^{-1} and the one for the analogous Ru(III) complex should be $\sim 10^{-5}$ s^{-1}, a difference in lability that was also found for substitutions on $Ru(NH_3)_5H_2O^{2+/3+}$ and aquations of $Ru(NH_3)_6^{3+/2+}$. Our preliminary directly determined values[12] for the water exchange on these hexaaquaions confirmed these estimates remarkably well.

The availability of stable solid salts of $Ru(H_2O)_6^{2+}$ has led to a variety of new compounds[13] since all six water molecules can easily be substituted. This is not the case for the complexes RuL_6^{2+} and $Ru(L\text{-}L)_3^{2+}$ (L, L-L = unsaturated ligand with low-lying π^* orbital(s)), which are known to be very stable and very inert due to a strong back-donation of electron density from the t_{2g} orbitals onto the ligand. This is best illustrated by the $Ru^{3+/2+}$ reduction potential of the $Ru(CH_3CN)_6^{2+}$ solvate (easily prepared from $Ru(H_2O)_6^{2+}$): no oxidation to the $Ru(CH_3CN)_6^{3+}$ solvate is observed in acetonitrile up to 2.5 V. This is not unreasonable, since a single acetonitrile ligand leads to a stabilization of the +2 oxidation state of ~0.4 V.[14]

In this paper we present a comprehensive study of the water exchange on $Ru(H_2O)_6^{2+}$ and $Ru(H_2O)_6^{3+}$ and of the acetonitrile exchange on $Ru(CH_3CN)_6^{2+}$. Mechanistic implications of the activation parameters ($\Delta H^{\ddagger}$, $\Delta S^{\ddagger}$, $\Delta V^{\ddagger}$) are discussed, and comparisons are made with other complexes and metal ions.

Experimental Section

Materials and Syntheses. Trifluoromethanesulfonic acid (Htrifl) was distilled at reduced pressure. *p*-Toluenesulfonic acid (Htos) (Fluka, puriss. p.a.), CH_3CN-d_3 (Ciba Geigy, 99.8% D), and oxygen-17 enriched water (Yeda, Israel) were used as received. $[Ru(H_2O)_6](trifl)_2$ and ^{17}O-labeled $[Ru(H_2O)_6](tos)_3 \cdot 3H_2O$ were prepared as reported.[15,16]

$[Ru(CH_3CN)_6](trifl)_2$. A 3.94-mmol amount of $[Ru(H_2O)_6](trifl)_2$ (2.0 g) was added to 25 mL of acetonitrile under argon. When heated to 80 °C, the solution turned yellow. When no further color change could be observed, the solution was stirred at 80 °C for an additional hour. A solid precipitate, which was formed upon cooling and rotatory concentration, was redissolved by gentle heating. Slow cooling to −20 °C produced faintly yellow needles, which were isolated by filtration and dried in vacuo. Yield: 80 %. Anal. Calcd (found) for $[Ru(CH_3CN)_6](CF_3SO_3)_2$: C, 26.05 (26.0); H, 2.81 (2.9); N, 13.02 (13.1); S, 9.93 (9.9); F, 17.66 (18.1); H_2O, 0 (<0.3). λ_{max} (ϵ_{max}): 375 nm (340 M^{-1} cm^{-1}), 270 nm (380 M^{-1} cm^{-1}).

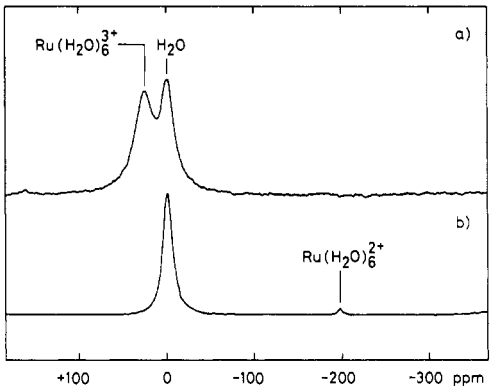

Figure 1. 27.11-MHz ^{17}O NMR spectra: (a) 0.3 *m* $[Ru(H_2{}^{17}O)_6](tos)_3$ (9% in ^{17}O) and 0.2 *m* Htos, at 301.9 K, about 200 min after mixing with normal water; (b) 0.25 *m* $[Ru(H_2O)_6](trifl)_2$ and 0.25 *m* Htrifl, at 297.7 K, isotopically equilibrated (5% oxygen-17) aqueous solution. The upper (lower) spectrum is the result of 7000 (670) scans using a repetition of 41 (10) ms and a pulse width of 15 (15) μs (90° pulse = 20 μs) in the quadratic detection mode; 2 (2) K data points were used over a total spectral width of 25000 (25000) Hz, and an exponential filter of 0 (50) Hz was used.

Instrumentation. Proton NMR spectra were recorded on a Bruker WP-60 spectrometer (1.4 T) working at 60 MHz, and oxygen-17 NMR spectra were obtained on a Bruker CXP-200 instrument that was equipped with a wide-bore cryomagnet (4.7 T) and was operated at 27.11 MHz.

The ambient-pressure kinetics were followed in commercial thermostated probe units, and the temperature was found constant within ±0.3 K as measured by a substitution technique.[17] For relatively fast exchange (10 s < $t_{1/2}$ < 1 h), a fast-injection apparatus described elsewhere[16] was used, whereas for very slow exchange ($t_{1/2}$ > 1 day), the samples were kept in thermostated baths and transferred at fixed intervals into the NMR probe to record spectra.

The high-pressure kinetics were performed in high-pressure probes described elsewhere (proton,[18] oxygen-17[19]). For very slow high-pressure exchanges, the samples, contained in deformable cylindrical thin-walled Teflon cells (8.5 mm o.d., 33 mm length), were kept in stainless-steel pressure vessels immersed in a thermostated bath. For the NMR measurements, the pressure was released, the Teflon cells introduced into 10-mm NMR tubes, the spectra measured, and, finally, the samples pressurized again. The time of this operation was short compared to the half-life of the exchange. Each kinetic run consisted of 15–30 spectra and was followed for 3–4 half-lives.

UV–visible spectra were obtained on a Perkin-Elmer Lambda 7 spectrophotometer with a 1-cm thermostated cell for variable-temperature measurements and with a 2-cm high-pressure optical cell[20] for variable-pressure experiments.

The pH was measured before and after the spectrophotometric measurement to ±0.02 pH with a glass electrode calibrated at pH 1.00 and 4.00.

Results

Water Exchange on $Ru(H_2O)_6^{2+}$. An oxygen-17 NMR spectrum of an isotopically equilibrated 0.25 *m* $Ru(H_2O)_6^{2+}$ aqueous solution (5% oxygen-17) recorded at 297.7 K is shown in Figure 1b. The resonance due to bound water was found at −196.3 ppm from the reference bulk water signal. No significant temperature dependence of the chemical shift was observed. At 297.7 K the

(5) Endicott, J. F.; Taube, H. *Inorg. Chem.* **1965**, *4*, 437.
(6) Matsubara, T.; Creutz, C. *J. Am. Chem. Soc.* **1978**, *100*, 6255; *Inorg. Chem.* **1979**, *18*, 1956.
(7) Broomhead, J. A.; Kane-Maguire, L. A. P.; Wilson, D. *Inorg. Chem.* **1975**, *14*, 2575, 2579.
(8) Fairhurst, M. T.; Swaddle, T. W. *Inorg. Chem.* **1979**, *18*, 3241.
(9) Lay, P. A.; Sasse, W. H. F. *Inorg. Chem.* **1985**, *24*, 4707.
(10) Bosnich, B.; Dwyer, F. P. *Aust. J. Chem.* **1966**, *19*, 2235.
(11) Kallen, T. W.; Earley, J. E. *Inorg. Chem.* **1971**, *10*, 1149.
(12) Bernhard, P.; Helm, L.; Rapaport, I.; Ludi, A.; Merbach, A. E. *J. Chem. Soc., Chem. Commun.* **1984**, 302.
(13) Bernhard, P.; Lehmann, H.; Ludi, A. *Comments Inorg. Chem.* **1983**, *3*, 145 and references therein. Bailey, O. H.; Ludi, A. *Inorg. Chem.* **1985**, *24*, 2582. Stebler-Röthlisberger, M.; Bürgi, H. B.; Salzer, A.; Ludi, A. *Organometallics* **1986**, *5*, 298.
(14) Clarke, R. E.; Ford, P. C. *Inorg. Chem.* **1970**, *9*, 227.
(15) Bernhard, P.; Bürgi, H.-B.; Hauser, J.; Lehmann, H.; Ludi, A. *Inorg. Chem.* **1982**, *21*, 3936.
(16) Bernhard, P.; Helm, L.; Ludi, A.; Merbach, A. E. *J. Am. Chem. Soc.* **1985**, *107*, 312.
(17) Ammann, C.; Meier, P.; Merbach, A. E. *J. Magn. Reson.* **1982**, *46*, 319.
(18) Earl, W. L.; Vanni, H.; Merbach, A. E. *J. Magn. Reson.* **1978**, *30*, 571.
(19) Pisaniello, D. L.; Helm, L.; Meier, P.; Merbach, A. E. *J. Am. Chem. Soc.* **1983**, *105*, 4520.
(20) Richens, D. T.; Ducommun, Y.; Merbach, A. E. *J. Am. Chem. Soc.* **1987**, *109*, 603.

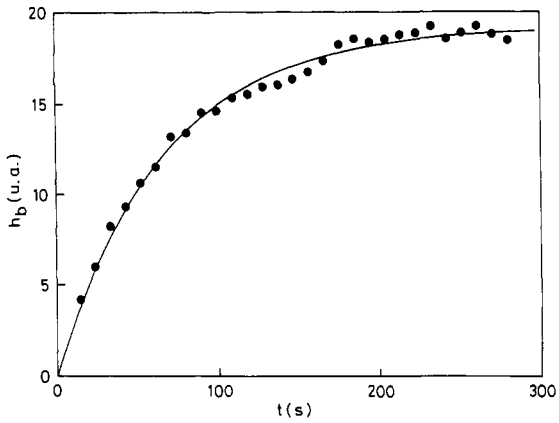

Figure 2. Height h_b, as a function of time, of the ^{17}O NMR signal of coordinated H_2O after addition of $Ru(H_2O)_6^{2+}$ to oxygen-17 enriched water (10%) at 297.7 K. (See caption for Figure 1b for experimental parameters.)

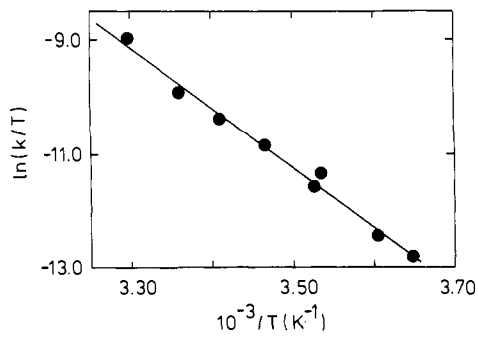

Figure 3. Eyring plot for the water exchange rate constants k (s^{-1}) for $Ru(H_2O)_6^{2+}$ in 0.25 m Htrifl.

transverse relaxation rates, $1/T_2$, obtained by line-width measurements ($1/T_2 = \pi(\Delta\nu_{1/2})$) are 980 s^{-1} for free and 372 s^{-1} for bound water. The bulk water signal was broadened by the presence of manganese(II) as impurity at trace level (the Mn:Ru:H_2O molar ratio is 1:5 × 10^2:1 × 10^5) as analyzed by inductively coupled plasma (ICP) emission spectroscopy. This impurity did not affect our measurements since the $Ru(H_2O)_6^{2+}$ signal was well separated from the bulk water signal.

The water exchange (eq 1) was followed as a function of temperature (274–303 K), after fast injection of 10% oxygen-17 enriched water (0.8 mL) into the same volume of an acidified

$$Ru(H_2O)_6^{2+} + 6H_2{}^{17}O \rightarrow Ru(H_2{}^{17}O)_6^{2+} + 6H_2O \quad (1)$$

solution of the aqua ion (0.5 m $[Ru(H_2O)_6](trifl)_2$ and 0.5 m Htrifl) under a nitrogen atmosphere. The rate law for isotopic exchange can be expressed by eq 2,[21] where k represents the rate

$$-dx/dt = k(x - x_\infty)/(1 - x_\infty) \quad (2)$$

constant for the exchange of a particular water molecule[22] and x and x_∞ represent the mole fractions of labeled water coordinated to the metal at the time of sampling and at exchange equilibrium, respectively. The increase in height h_b of the small signal from coordinated oxygen-17 water with time was used to monitor the exchange kinetics. Because of the low $Ru(H_2O)_6^{2+}$ concentration used and the good stability of the spectrometer electronics, the intensity of the large bulk water signal was not noticeably modified. The heights h_b (proportional to x) were measured with a ruler and fitted, with $h_{b\infty}$ and k as adjustable parameters, to eq 3,

$$h_b = h_{b\infty}[1 - \exp(-kt/(1 - x_\infty))] \quad (3)$$

obtained by integration of eq 2 with $x = 0$ at $t = 0$ and $x_\infty \approx 6 \times 0.25/55 \approx 0.03$. Figure 2 shows a typical example of a kinetic run. The water exchange rate constants obtained in this way, as

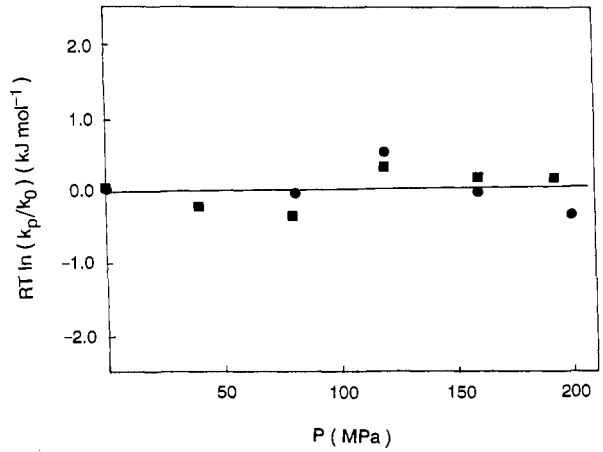

Figure 4. Effect of pressure on the water exchange rate constant k (s^{-1}) for $Ru(H_2O)_6^{2+}$ in 1.5 m Htrifl at 268.2 (●) and 273.3 K (■).

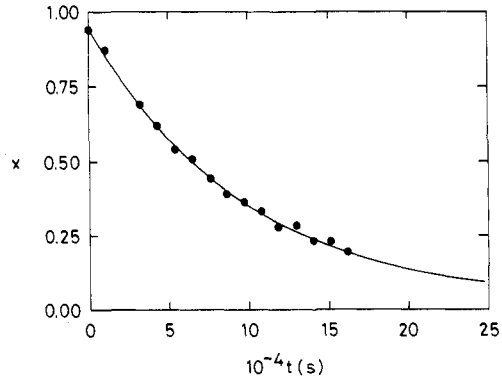

Figure 5. Mole fraction x of bound CH_3CN, as a function of time, as monitored by ^1H NMR, after dissolution of $[Ru(CH_3CN)_6](trifl)_2$ in CH_3CN-d_3 at 372.8 K ($[Ru^{2+}]$ = 0.1 m).

well as the transverse relaxation rate (quadrupolar mechanism), were least-squares fitted to eq 4 (Figure 3) and 5, respectively,

$$k = (k_B T/h) \exp(\Delta S^\ddagger/R - \Delta H^\ddagger/RT) \quad (4)$$

$$1/T_{2Q}{}^b = 1/T_{2Q}{}^{b,298} \exp[E_Q{}^b/R(1/T - 1/298.15)] \quad (5)$$

leading to $k^{298} = (1.8 \pm 0.2) \times 10^{-2}$ s^{-1}, $\Delta H^\ddagger = 87.8 \pm 4$ kJ mol^{-1}, $\Delta S^\ddagger = +16.1 \pm 15$ J K^{-1} mol^{-1}, $1/T_{2Q}{}^{b,298} = 378 \pm 9$ s^{-1}, and $E_Q{}^b = 16.0 \pm 1.1$ kJ mol^{-1}. Although solutions at three different acidities (0.025, 0.25, 1.50 m) were studied at 283.7 K, no acid dependence could be detected, indicating that no hydrolytic pathway for water exchange is effective at acidities higher than 0.025 m.

Two series of variable-pressure measurements were carried out at 268 and 273 K. To minimize the exchange during the mixing at ambient pressure, acidified 10% oxygen-17 enriched water and the same volume of an acidified aqua ion solution (0.5 m $[Ru(H_2O)_6](trifl)_2$) were mixed at 258 K before introduction into the thermostated high-pressure probe and pressurization. The whole procedure took about 5 min. The two sets of rate constants (for the two temperatures) were simultaneously fitted to eq 6, leading

$$\ln k_P = \ln k_0 - \Delta V^\ddagger P/RT \quad (6)$$

to $\Delta V^\ddagger = -0.4 \pm 0.7$ cm^3 mol^{-1}, $k_0{}^{268} = (3.1 \pm 0.3) \times 10^{-4}$ s^{-1}, and $k_0{}^{273} = (6.2 \pm 0.5) \times 10^{-4}$ s^{-1}. The experimental and calculated rate constants k_P, normalized to the exchange rate constants k_0 (at atmospheric pressure), are shown in Figure 4. A similar least-squares fit of the transverse relaxation rates to eq 7 gave $\Delta V^\ddagger{}_b = +0.9 \pm 0.8$ cm^3 mol^{-1}, $(1/T_2{}^b)_0{}^{268} = 947 \pm 51$ s^{-1},

$$\ln (1/T_2{}^b)_P = \ln (1/T_2{}^b)_0 - \Delta V^\ddagger{}_b P/RT \quad (7)$$

and $(1/T_2{}^b)_0{}^{273} = 901 \pm 43$ s^{-1}.

Acetonitrile Exchange on $Ru(CH_3CN)_6^{2+}$. This exchange reaction (eq 8) was followed by monitoring the increase in intensity

(21) Helm, L.; Elding, L. I.; Merbach, A. E. *Inorg. Chem.* **1985**, *24*, 1719.
(22) Swaddle, T. W. *Adv. Inorg. Bioinorg. Mech.* **1983**, *2*, 95.

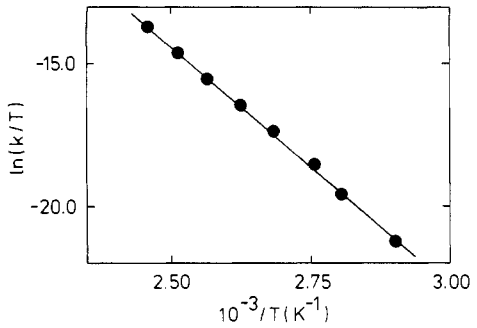

Figure 6. Eyring plot for the acetonitrile exchange rate constant k (s^{-1}) for $Ru(CH_3CN)_6^{2+}$ in neat solvent.

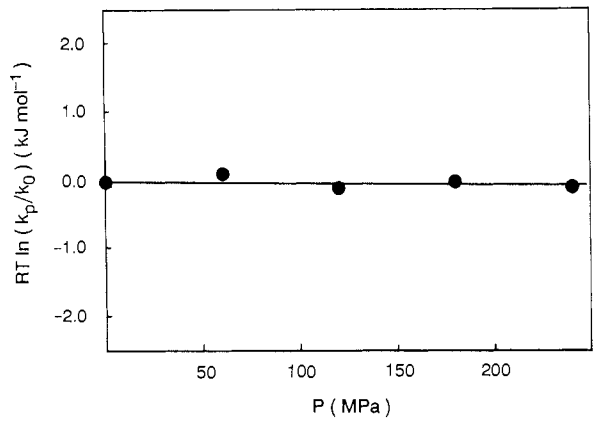

Figure 7. Effect of pressure on the acetonitrile exchange rate constant k (s^{-1}) for $Ru(CH_3CN)_6^{2+}$ in neat solvent at 362.9 K.

of the proton NMR signal of free CH_3CN (at +2.00 ppm from TMS) and the decrease of the bound CH_3CN (at +2.59 ppm),

$$Ru(CH_3CN)_6^{2+} + 6CH_3CN\text{-}d_3 \rightarrow Ru(CH_3CN\text{-}d_3)_6^{2+} + 6CH_3CN \quad (8)$$

after dissolution of $[Ru(CH_3CN)_6](trifl)_2$ in deuteriated acetonitrile. The time dependence of the mole fraction x of bound acetonitrile, obtained by integration of the signals (Figure 5) was fitted to eq 9, resulting from integration of eq 2 with $x = x_0$ at

$$x = x_\infty + (x_0 - x_\infty)\exp[-kt/(1 - x_\infty)] \quad (9)$$

$t = 0$ and $x_\infty \approx 6 \times 0.1/24 \simeq 0.02$. The adjustable parameters were k and x_0. The exchanges were followed directly in the NMR probe heads, except for the two slowest, at 344.9 and 356.7 K, where the samples were kept in thermostated baths and NMR analyzed at fixed intervals at ambient temperature. The variable-temperature (Figure 6) and variable-pressure at 362.9 K (Figure 7) rate constants were fitted to eq 4 and 6, respectively, leading to $k^{298} = (8.9 \pm 2) \times 10^{-11}$ s^{-1}, $\Delta H^{\ddagger} = 140.3 \pm 2$ kJ mol^{-1}, $\Delta S^{\ddagger} = +33.3 \pm 6$ J K^{-1} mol^{-1}, $k_0^{363} = (3.2 \pm 0.1) \times 10^{-6}$ s^{-1}, and $\Delta V^{\ddagger} = +0.4 \pm 0.6$ cm^3 mol^{-1}.

Water Exchange on $Ru(H_2O)_6^{3+}$. Figure 1a shows the oxygen-17 NMR spectrum of an acidified 0.3 m $Ru(H_2O)_6^{3+}$ aqueous solution obtained at 301.9 K, about 200 min after the oxygen-17 enriched aqua ion (9%) was mixed with normal water. The two overlapping signals were fitted to two Lorentzians in order to obtain their shifts, line widths, and integrals. The bound water signal at +34.7 ppm (shift only slightly temperature and acidity dependent) decreased while the bulk water signal increased (shift reference) with time. For comparison the bound water shifts of the diamagnetic Ru^{2+} and Rh^{3+} ions are −196.3 and −130.5 ppm,[23] respectively. Therefore the small shift observed for $Ru(H_2O)_6^{3+}$ is probably due to a paramagnetic high-frequency contribution. The transverse relaxation rates of bound and free water were 2130 and 1430 s^{-1}, respectively. Again the bulk water signal was broadened by traces of manganese(II) (no effect on the exchange kinetics). The line width of the water coordinated to the low-spin t_{2g}^5 Ru^{3+} ion is small for a paramagnetic ion and is comparable to those of trivalent diamagnetic hexaaquaions ($1/T_{2Q}$[b]:2297 s^{-1} for Al^{3+}, 1567 s^{-1} for Ga^{3+}),[24,25] implying that the quadrupolar relaxation mechanism is dominant. The ^{17}O relaxation rate for the bound water increased with increasing acidity (increasing ionic strength) but decreased rapidly with increasing temperature as anticipated for the quadrupolar relaxation mechanism. At temperatures higher than 310 K, a smaller decrease of $1/T_2$ was observed because the scalar interaction with the electronic spin of this ion becomes more important.[26]

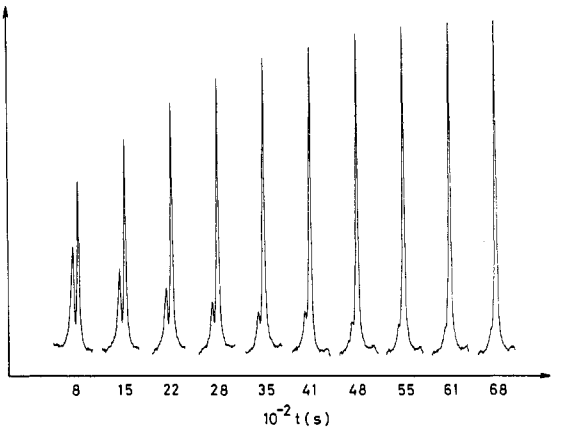

Figure 8. 27.11-MHz ^{17}O NMR spectra, as a function of time at 315.3 K, of a 0.3 m $[Ru(H_2{}^{17}O)_6](tos)_3$ (9% ^{17}O) and 0.5 m Htos aqueous solution obtained after mixing with normal water (for spectral assignment, see Figure 1a).

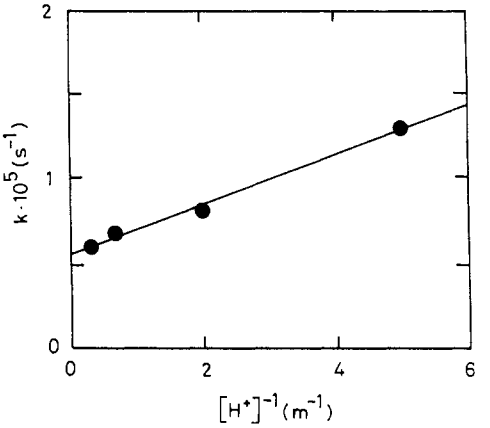

Figure 9. Acid dependence of the total water exchange rate constant k (s^{-1}) for 0.3 m $Ru(H_2O)_6^{3+}$ at 301.9 K.

The exchange (eq 10) was followed by monitoring the depletion of the hexaaquaion and the enrichment of bulk water in oxygen-17 (Figure 8). The initial intensity of the free water peak is larger

$$Ru(H_2{}^{17}O)_6^{3+} + 6H_2O \rightarrow Ru(H_2O)_6^{3+} + 6H_2{}^{17}O \quad (10)$$

than expected for normal water, due to the labile water of crys-

(23) Rapaport, I.; Laurenczy, G.; Zbinden, D.; Merbach, A. E., to be submitted for publication.

(24) Hugi-Cleary, D.; Helm, L.; Merbach, A. E. *Helv. Chim. Acta* **1985**, *68*, 545.

(25) Hugi-Cleary, D.; Helm, L.; Merbach, A. E. *J. Am. Chem. Soc.* **1987**, *109*, 4444.

(26) The bound water oxygen-17 relaxation rate is the sum of three contributions: $1/T_2 = 1/T_{2Q} + 1/T_{2SC} + 1/T_{2DD}$. For oxygen-17 the last contribution is always small and the second one is related to the electron relaxation rate $1/T_e$ by

$$1/T_{2SC} = \tfrac{1}{3}S(S+1)(2\pi A/h)^2\,\tau_s[1 + 1/(1 + \omega_s^2\tau_s^2)]$$

with $\tau_s \approx T_e$ since the electronic relaxation rate $1/T_e$ for an orbitally degenerate ground state ($^2T_{2g}$ for Ru^{3+}) is particularly fast (and for a second-row transition metal with a large spin–orbit coupling constant even more so), it follows that $1/T_{2SC}$ must be small as observed.

Table I. Water Exchange Rate Constant of $Ru(H_2O)_6^{3+}$ as a Function of Temperature and Acidity[a]

[Htos], m	$10^6k/s^{-1}$ T = 288.2 K	T = 301.9 K	T = 315.3 K	T = 328.6 K
0.2	2.13 ± 0.04	13.0 ± 0.2	174 ± 5	1039 ± 29
0.5	1.36 ± 0.04	8.1 ± 0.1	86 ± 2	487 ± 15
1.5	1.04 ± 0.04	6.8 ± 0.1	41 ± 1	255 ± 4
3.0	1.01 ± 0.03	6.0 ± 0.2	31 ± 1	203 ± 5

[a] The concentration of $[Ru(H_2O)_6](tos)_3$ was 0.30 *m*, and its initial ^{17}O enrichment was 9%.

Table II. Water Exchange Rate Constant of $Ru(H_2O)_6^{3+}$ as a Function of Pressure and Acidity at 288.2 K[a]

[Htos], m	$10^6k/s^{-1}$ P = 0.1 MPa	P = 70 MPa	P = 140 MPa	P = 210 MPa
0.1	4.6 ± 0.5	5.2 ± 0.4	5.9 ± 0.7	6.5 ± 0.4
0.5	1.6 ± 0.1	1.9 ± 0.1	2.5 ± 0.3	2.8 ± 0.2
3.0	1.2 ± 0.1	1.8 ± 0.2	2.3 ± 0.1	2.6 ± 0.4

[a] The concentration of $[Ru(H_2O)_6](tos)_3$ was 0.15 *m*, and its initial ^{17}O enrichment was 27%.

tallization present in the hexaaquaruthenium(III) tosylate salt. The time dependence of the mole fraction of bound oxygen-17 water, obtained from the fitted integrals, was fitted to eq 9. The adjustable parameters were k and x_0, the latter being related to the number of water molecules of crystallization n through eq 11,

$$n = (6/x_0) - (2.06 \times 10^{-2}/mc) - 6 \quad (11)$$

where m is the molality and c is the oxygen-17 content of the aqua ion. The average value, $n = 2.6 \pm 0.2$, agrees well with the literature value of three water molecules of crystallization.[15] As already found for other trivalent aquaions,[25] the exchange rate k shows a strong acid dependence (Figure 9) that can be split into two contributions according to eq 12, k_1 being the rate for water

$$k = k_1 + k_2/[H^+] \quad (12)$$

exchange on $Ru(H_2O)_6^{3+}$ and k_2 being the product (eq 13) of k_{OH},

$$k_2 = k_{OH}K_a \quad (13)$$

$$Ru(H_2O)_6^{3+} \rightleftharpoons Ru(H_2O)_5OH^{2+} + H^+ \quad (14)$$

the rate constant for water exchange on the monohydroxy species and K_a the first hydrolysis constant for $Ru(H_2O)_6^{3+}$ (eq 14). All six oxygen atoms in $Ru(H_2O)_5OH^{2+}$ were assumed to contribute equally to the observed k_2 value. In the iron(III) case Grant and Jordan[27] assumed that the hydroxo ligand does not contribute to the exchange and applied a factor of $^5/_6$ to the rate coefficients accordingly. Arguably, a statistical factor of $^1/_6$ should be applied if the hydroxo ligand activates the trans water specifically, but there is no direct evidence for this. These considerations do not affect the calculation of either volumes or enthalpies of activation.[28] The variable-temperature rate constants obtained at four acid concentrations and four temperatures (Table I) were least-squares fitted to eq 4 and 12, leading to $k_1^{298} = (3.5 \pm 0.3) \times 10^{-6}$ s^{-1}, $\Delta H_1^* = 89.8 \pm 4$ kJ mol^{-1}, and $\Delta S_1^* = -48.3 \pm 14$ J K^{-1} mol^{-1} and $k_2^{298} = (1.1 \pm 0.2) \times 10^{-6}$ *m* s^{-1}, $\Delta H_2^* = 136.9 \pm 6$ kJ mol^{-1}, and $\Delta S_2^* = +100.5 \pm 18$ J K^{-1} mol^{-1}. The variable-pressure data, obtained at three acidities and four pressures at 288.2 K (Table II) and least-squares fitted to eq 6 and 12, gave $k_{1,0}^{288} = (1.1 \pm 0.2) \times 10^{-6}$ s^{-1} and $\Delta V_1^* = -8.3 \pm 2.1$ cm^3 mol^{-1} and $k_{2,0}^{288} = (0.35 \pm 0.03) \times 10^{-6}$ *m* s^{-1}, $\Delta V_2^* = -2.1 \pm 1.4$ cm^3 mol^{-1}.

Acid Dissociation of $Ru(H_2O)_6^{3+}$. The pK_a of $Ru(H_2O)_6^{3+}$ (eq 14) has been previously determined spectrophotometrically (2.4 ± 0.1)[29] and electrochemically (2.9)[30] at 298.2 K, by measuring the intense absorption band of $Ru(H_2O)_5OH^{2+}$ at 288 nm and the redox potential, respectively, as a function of pH. The former measurement was first repeated on a 3.0×10^{-4} *m* ruthenium(III) solution at 298.2 K and 290 nm. The dependence of the absorbance A upon pH is given by eq 15, where b (cm) is the optical

$$A = b[Ru(III)][\epsilon_{Ru^{3+}} + \epsilon_{RuOH^{2+}}10^{pH-pK_a}]/(1 + 10^{pH-pK_a}) \quad (15)$$

path length and $\epsilon_{Ru^{3+}}$ and $\epsilon_{RuOH^{2+}}$ (m^{-1} cm^{-1}) the molar absorptivities of the species in equilibrium. A least-squares fit of the experimental A values to eq 15 with pK_a, $\epsilon_{Ru^{3+}}$ and $\epsilon_{RuOH^{2+}}$ as adjustable parameters gave 2.60 ± 0.08, 143 ± 30, and 1307 ± 70, respectively. The pK_a value is in agreement with the above reported values.

A series of variable-temperature experiments were performed on a solution of pH 2.45 between 275.3 and 312.9 K (the contribution to $[H^+]$ from the dissociation of $Ru(H_2O)_6^{3+}$ is negligible since $[Ru(H_2O)_6^{3+}] \ll [CF_3SO_3H]$; therefore, essentially no temperature dependence is expected for the pH). Above this upper temperature, rapid oligomerization is taking place as shown from the UV–vis spectra.[29] The pK_a values, deduced from absorbance changes with temperature (Table III), were fitted to eq 16, giving

$$pK_a = (1/2.303R)[(\Delta H_a^0/T) - \Delta S_a^0] \quad (16)$$

$pK_a^{298} = 2.73 \pm 0.02$, $\Delta H_a^0 = 41.1 \pm 1.9$ kJ mol^{-1}, and $\Delta S_a^0 = 85.6 \pm 6.4$ J K^{-1} mol^{-1}.

A series of variable-pressure experiments, up to 190 MPa at 278.0 K, were performed on a solution of pH 2.60. The pK_a values obtained from absorbance changes with pressure (Table III) were fitted to eq 17, yielding $\Delta V_a^0 = -3.0 \pm 0.6$ cm^3 mol^{-1} and $pK_a^0 = 3.24 \pm 0.01$.

$$pK_a = pK_a^0 + \Delta V_a^0 P/2.303RT \quad (17)$$

Combining ΔV_a^0 and ΔV_2^* (−2.1 cm^3 mol^{-1}), the experimental volume of activation, one obtains ΔV_{OH}^*, the volume of activation for the water exchange on the $Ru(H_2O)_5(OH)^{2+}$ species: $\Delta V_{OH}^* = \Delta V_2^* - \Delta V_a^0 = +0.9$ cm^3 mol^{-1}.

Table III. Temperature and Pressure Dependence of A, Measured at 290 nm, and Corresponding pK_a, Obtained from a 3.0×10^{-4} *m* $[Ru(H_2O)_6](tos)_3$ Aqueous Solution ($\mu = 2.00$ *m* (Na(trifl)))

variable temp T/K	A	pK_a	variable pressure (at 278.0 K) P/MPa	A	pK_a
275.3	0.087	3.29	0.1	0.213	3.24
283.6	0.105	3.11	40	0.220	3.21
291.2	0.129	2.93	70	0.221	3.21
298.2	0.160	2.75	100	0.226	3.19
305.0	0.192	2.56	130	0.227	3.19
312.9	0.236	2.36	160	0.232	3.17
			190	0.248	3.11

Table IV. Rate Constants and Activation Parameters for Solvent Exchange on RuS_6^{2+} in Neat Solvent

S	k^{298}/s^{-1}	ΔH^*/kJ mol^{-1}	ΔS^*/J mol^{-1} mol^{-1}	ΔV^*/cm^3 mol^{-1}
H_2O	$(1.8 \pm 0.2) \times 10^{-2}$	87.8 ± 4	+16.1 ± 15	−0.4 ± 0.7
CH_3CN	$(8.9 \pm 2) \times 10^{-11}$	140.3 ± 2	+33.3 ± 6	+0.4 ± 0.6

Discussion

High-pressure multinuclear magnetic resonance has proven an invaluable technique in the study of solvent exchange on metal ions, reactions which are fundamental to the understanding of substitution and redox reactions in inorganic chemistry.[31] For these exchange reactions, characterized by symmetrical pathways and no major electrostrictive changes to reach the transition state, the acceleration or the retardation of the exchange rate constant with pressure is unambiguously related to the activation mode—dissociative or associative—for a positive or a negative activation volume, respectively. The most striking and at the time unexpected

(27) Grant, M.; Jordan, R. B. *Inorg. Chem.* **1981**, *20*, 55.
(28) Swaddle, T. W.; Merbach, A. E. *Inorg. Chem.* **1981**, *20*, 4212.
(29) Harzion, Z.; Navon, G. *Inorg. Chem.* **1980**, *19*, 2236.
(30) Böttcher, W.; Brown, G. M.; Sutin, N. *Inorg. Chem.* **1979**, *18*, 1447.
(31) *Inorganic High Pressure Chemistry:Kinetics and Mechanisms*; van Eldik, R., Ed.; Elsevier: Amsterdam, 1986.

Table V. Rate Constants and Activation Parameters for Water Exchange on Hexaaqua- and Hydroxypentaaquametal Ions

	k^{298}/s^{-1}	k_{OH}/k_1	$\Delta H^{\ddagger}$/kJ mol^{-1}	$\Delta S^{\ddagger}$/J K^{-1} mol^{-1}	$\Delta V^{\ddagger}$/cm^3 mol^{-1}	pK_a	ref
Ga^{3+}	4.0×10^2	275	67.1	+30.1	+5.0	~3.9	25
$Ga(OH)^{2+}$	1.1×10^5		58.9		+6.2		
Fe^{3+}	1.6×10^2	750	64.0	+12.1	−5.4	2.9	27,28
$Fe(OH)^{2+}$	1.2×10^5		42.4	+5.3	+7.0		
Cr^{3+}	2.4×10^{-6}	75	108.6	+11.6	−9.6	4.1	37
$Cr(OH)^{2+}$	1.8×10^{-4}		110.0	+55.6	+2.7		
Ru^{3+}	3.5×10^{-6}	170	89.8	−48.3	−8.3	2.7	this work
$Ru(OH)^{2+}$	5.9×10^{-4}		95.8	+14.9	+0.9		

results were obtained for divalent and trivalent hexasolvated high-spin first-row transition-metal ions: for both oxidation states a gradual changeover in substitution mechanisms occurs along the series in water, methanol, and acetonitrile media, with the early members showing associative activation mode and the later ones dissociative behavior, the change in activation mode occurring after the d^5 configuration.[32] This mechanism changeover has been rationalized in terms of decreasing cationic size and filling of the 3d orbitals along the series, both disfavoring associative activation modes.

Results concerning simple solvent exchange and complex formation reactions on octahedrally coordinated second-row transition-metal ions are far more scarce and show associative behavior: complex formations in water between Mo^{3+} and NCS^-,[20] Cd^{2+} and bpy (2,2′-bipyridine);[33] trimethyl phosphate (TMP) exchange on In^{3+}.[32] The two latter reactions can be used for a direct comparison with those of the first-row analogues. For the trivalent closed d shell Ga^{3+} and In^{3+} ions, a drastic difference in mechanism has been observed for the TMP exchange on the $M(TMP)_6^{3+}$ species: dissociative D mechanism for the smaller ion (for Ga^{3+}, r_i = 62 pm and ΔV = +20.7 cm^3 mol^{-1}); associative A, or associative interchange I_a, mechanism for the larger ion (for In^{3+}, 80 pm and −21.4 cm^3 mol^{-1}).[32] A similar difference has also been observed between the first and second rows for divalent metal ions: an I_d mechanism has been ascribed for the complex formation reaction between $Zn(H_2O)_6^{2+}$ and bpy (r_i = 74 pm and $\Delta V_f^{\ddagger}$ = +7.1 cm^3 mol^{-1}), whereas an I_a mechanism has been assigned to the same reaction with $Cd(H_2O)_6^{2+}$ (95 pm and −5.5 cm^3 mol^{-1}).[33] At first glance one would therefore expect an associative substitution behavior for all the divalent and trivalent hexacoordinated second-row transition-metal ions. However, spin pairing, which is the rule along this series, will produce smaller ionic radii and therefore less associative behavior than expected. The solvated low-spin Ru^{2+} and Ru^{3+} ions in water and acetonitrile are typical in this respect.

The relative inertness of the Ru^{2+} and Ru^{3+} solvates did not allow us to use the classical NMR line-broadening technique[32] for their kinetic study; instead, the isotopic labeling method was used, employing ^1H and ^{17}O NMR to trace the solvent exchange. Accurate rate constants were obtained from fits of signal intensities to first-order equations; therefore, no assumptions about relaxation mechanisms had to be made as is often the case with line-broadening techniques. Also the parameters describing the quadrupolar relaxation of the ^{17}O nucleus are of no importance here, except that they are in good agreement with the ones previously reported.[16] The definitive advantage of NMR spectroscopy over mass spectrometry is that both the different possible kinetic processes and the possible formation of side products can easily be discerned from the spectra without previous chemical transformations.

For ruthenium(II) the conclusion obtained from the high-pressure data is that both water and acetonitrile exchange are taking place via an interchange I mechanism. The volumes of activation, zero within experimental errors (Table IV), are indicative of equal contributions from bond making and bond breaking in the formation of the transition state.[32] Ru^{2+} has an ionic radius of 73 pm[15] and a t_{2g}^6 electronic configuration. It is of interest to compare its behavior with that of the analogous first-row Fe^{2+} (78 pm, $t_{2g}^4e_g^2$, $\Delta V^{\ddagger}$ = +3.8 cm^3 mol^{-1} for water exchange).[28] In this comparison two opposite effects are operative: (i) the increase in ionic radius from Ru^{2+} to Fe^{2+} should increase the associative character; (ii) the presence of two electrons in the e_g σ-antibonding orbitals, should favor dissociation. Apparently this second effect predominates as indicated by the smaller activation volume for Ru^{2+} than for Fe^{2+}. Further the Ru^{2+} behavior can be compared to those of Co^{2+} (74 pm, $t_{2g}^5e_g^2$, +6.1 cm^3 mol^{-1}) and Ni^{2+} (69 pm, $t_{2g}^6e_g^2$, +7.2 cm^3 mol^{-1}).[34] From its intermediate ionic radius alone one would also have expected an I_d mechanism for Ru^{2+}; its I behavior is due to the predominance of dissociation for e_g vs. t_{2g} filling as discussed above.

The difference of 8 orders of magnitude between the water and acetonitrile exchange rates (Table IV) is reflected almost exclusively in the enthalpy of activation. Undoubtedly the inertness of $Ru(CH_3CN)_6^{2+}$ results from the great thermodynamic stability of the complex; responsible for this is the very strong back-bonding[35] from the electron-rich t_{2g}^6 Ru^{2+} ion into the π^* orbital of the coordinated acetonitrile. This effect has been well documented elsewhere.[36] There is no such back-bonding possible in $Ru(H_2O)_6^{2+}$.

For $Ru(H_2O)_6^{3+}$, the distinctly negative volume and entropy of activation (Table V) lead us to the conclusion that the water exchange is following an associative pathway; whether it is I_a or A requires discussion of the magnitude of $\Delta V^{\ddagger}$. Its value is significantly less negative than that calculated for an associative A mechanism (−13.9 cm^3 mol^{-1}) from Swaddle's model[38] and, more important, clearly less negative than the most negative experimental value (Ti^{3+}, −12.1 cm^3 mol^{-1}).[39] The assignment of an associative interchange I_a mechanism is therefore appropriate in the present case. The water exchange mechanism on the hexaaqua Ru^{3+} (68 pm, t_{2g}^5) can be compared with those on the two first-row ions Ti^{3+} (67 pm, t_{2g}^1)[38] and Fe^{3+} (64 pm, $t_{2g}^3e_g^2$, −5.4 cm^3 mol^{-1}).[27,28] In the first case the radii are similar, but the larger electronic population on Ru^{3+} disfavors the approach of a seventh solvent molecule at the transition state, diminishing the associative character compared to that with Ti^{3+}. In the second case both the decrease in ionic radius and the filling of e_g instead of t_{2g} orbitals on going to Fe^{3+} explains the larger dissociative character of the latter.

For Ga^{3+}, Fe^{3+}, Cr^{3+}, and the low-spin Ru^{3+} in water, hydrolysis is kinetically important and the conjugate base is in equilibrium with the hexaaquaion (eq 14), offering an alternative pathway for water exchange. Two main features are apparent from the rate constant and activation parameters reported in Table V: a higher reactivity (by a factor of 75–750) and a larger dissociative character (more positive activation volumes) for water exchange on the monohydroxypentaaqua metal ions. This drastic mechanistic difference between both exchange pathways is due to the strong electron-donating capability of HO^-. The strong bonding between the metal center and this group will weaken the remaining metal–water bonds, most probably the trans one. The complex thus becomes more labile, and dissociative activation is favored.

(32) Merbach, A. E. *Pure Appl. Chem.* **1982**, *54*, 1479; **1987**, *59*, 16.
(33) Ducommun, Y.; Laurenczy, G.; Merbach, A. E. *Inorg. Chem.*, in press.
(34) Ducommun, Y.; Newman, K. E.; Merbach, A. E. *Inorg. Chem.* **1980**, *19*, 3696.
(35) Chatt, J.; Duncanson, L. A. *J. Chem. Soc.* **1953**, 2939.
(36) Gress, M. E.; Creutz, C.; Quicksall, C. O. *J. Am. Chem. Soc.* **1981**, *103*, 981. Lehmann, H.; Schenk, K. J.; Chapuis, G.; Ludi, A. *J. Am. Chem. Soc.* **1979**, *101*, 6197.
(37) Xu, F.-C.; Krouse, H. R.; Swaddle, T. W. *Inorg. Chem.* **1985**, *24*, 267.
(38) Swaddle, T. W. *Inorg. Chem.* **1983**, *22*, 2663.
(39) Hugi, A. D.; Helm, L.; Merbach, A. E. *Inorg. Chem.* **1987**, *26*, 1763.

In the iron(III) case the mechanistic change is most pronounced: from I_a for $Fe(H_2O)_6^{3+}$ to I_d for $Fe(H_2O)_5(OH)^{2+}$. In $Ru(H_2O)_6^{3+}$ the associative character is stronger; therefore, the mechanistic change toward dissociation is less pronounced in $Ru(H_2O)_5(OH)^{2+}$. At the transition state both bond making and bond-breaking (I mechanism) contribute equally to the activation volume.

Acknowledgment. We thank the Swiss National Science Foundation for financial support (Grants 2.854-0.85 and 2.209-0.81) and CIBA-GEIGY AG for elemental analyses.

Registry No. $Ru(H_2O)_6^{2+}$, 30251-71-9; $Ru(H_2O)_6^{3+}$, 30251-72-0; $Ru(H_2O)_5OH^{2+}$, 73663-64-6; $Ru(CH_3CN)_6^{2+}$, 53139-84-7; H_2O, 7732-18-5; CH_3CN, 75-05-8.

Supplementary Material Available: Water exchange rate constants and oxygen-17 quadrupolar relaxation rates of $Ru(H_2O)_6^{2+}$ as a function of temperature (Table SI) and pressure (Table SII), acetonitrile exchange rate constants of $Ru(CH_3CN)_6^{2+}$ as a function of temperature and pressure (Table SIII), oxygen-17 transverse relaxation rates of $Ru(H_2O)_6^{3+}$ as a function of temperature and acidity (Table SIV), and pH dependence of the absorbance of a $Ru(H_2O)_6^{3+}$ solution (Table SV) (4 pages). Ordering information is given on any current masthead page.

Contribution from the Institute of Inorganic Chemistry, Technical University of Aachen, D-5100 Aachen, FRG, and Institute of Physical Chemistry II, Ecole Polytechnique Fédérale de Lausanne, CH-1015 Lausanne, Switzerland

Kinetics and Mechanism of the Reduction of Protons to Hydrogen by Cobaltocene

U. Koelle,*† P. P. Infelta,‡ and M. Grätzel‡

Received February 2, 1987

The rate constant k_{obsd} for the overall reaction $2CoCp_2 + 2H^+ \rightarrow 2CoCp_2^+ + H_2$ (eq i) was determined by pulse radiolysis in an aqueous sulfuric acid medium for cobaltocene (**1**), 1,2,3,4,5-pentamethylcobaltocene (**2**), and decamethylcobaltocene (**3**). The reaction is first order in **1** and in protons with $k_{2,obsd} = 42 \pm 1.5\ s^{-1}\ M^{-1}$ at $c_{H^+} = 8 \times 10^{-3}$–$4.7 \times 10^{-1}$ M. Possible mechanistic pathways for eq i are discussed, and a second-order disproportionation of protonated **1** or a mechanism that involves reduction of protonated **1** by unprotonated **1** is best compatible both with the observed kinetics and with chemical evidence. Deuteriation experiments show protonation to occur exclusively at the metal.

Introduction

From the beginning of cobaltocene chemistry one of the most intriguing reactions of this electron-rich sandwich complex has been the one with acids.[1,2] Reports from different laboratories noted a somewhat different course of the reaction depending on the acid employed. Thus, whereas aqueous HCl led to the formation of a tetrachlorocobaltate with partial decomplexation of Co (eq 1),[3] a clean oxidation of **1** to 1^+ with acids having a noncoordinating anion such as HBF_4 and HPF_6 was found.[4] We observed that also acids like H_2SO_4, CH_3COOH, and CF_3COOH in water and polar organic solvents exclusively reacted according to eq 2. Reaction 2 is of interest as a model reaction for the

$$\underset{\mathbf{1}}{3CoCp_2} + 4\,HCl \rightarrow \underset{\mathbf{1^+}}{[CoCp_2]_2CoCl_4} + H_2 + 2CpH \quad (1)$$

$$2CoCp_2 + 2HX \rightarrow 2[CoCp_2]X + H_2 \quad (2)$$

$$X = BF_4^-,\ PF_6^-,\ HSO^-,\ \text{etc.}$$

reduction of protons by a transition-metal complex. Since it is a noncomplementary electron-transfer reaction, its mechanism must be complex. Visually the reaction of **1** with 0.1 M HBF_4, H_2SO_4, or CF_3COOH in THF/water is complete in the time of mixing at ambient temperature without noticeable formation of intermediates.

Evaluation of the kinetics of reaction 2 faces two major problems. Since the kinetics are too fast to be followed by conventional spectrophotometry, the air sensitivity of cobaltocene at the low concentrations available in water (estimated 10^{-5} M) precludes its handling in all but rigorously closed systems. Since oxidations by protons or oxygen are spectrophotometrically indistinguishable, minor traces of oxygen would interfere with the kinetics. These difficulties are overcome by reducing the cobaltocenium cation 1^+ with electrons or reducing radicals, generated in an electron pulse, in acidic aqueous solution to neutral cobaltocene and monitoring the absorption decay of the latter when reaction 2 proceeds.

In addition to the pulse radiolysis experiments performed along these lines, results of the oxidation of **1** and its 1,2,3,4,5-pentamethyl derivative, **2**, by CH_3COOH in ethanol, monitored by using conventional spectrophotometry, are presented. The reaction of **1** with CF_3COOD in CH_3OD was studied to probe the site of protonation.

Experimental Section

For **electrochemical** measurements EG&G/PAR equipment (Model 173 potentiostat/galvanostat and Model 174A polarographic analyzer) was used. Cyclic voltammograms in ethanol/H_2SO_4/Na_2SO_4 were recorded on a hanging-mercury-drop electrode (EG&G/PAR SMDE 303). Bulk electrolysis of 1^+ was performed in a divided cell at a mercury-pool cathode. The electrolyte consisted of an aqueous surfactant solution (4×10^{-3} M $C_nF_{2n+1}SO_3H$[5]) and 0.1 M $LiClO_4$ as the supporting electrolyte.

Samples for **pulse radiolysis** were prepared by Ar-degassing (1–5) $\times 10^{-3}$ M aqueous solutions of [**1**–**3**]Cl in 1 × 1 cm quartz cells fitted with gastight rubber septums and containing varying concentrations of sulfuric acid and 10% v/v of 2-propanol.[6] The cells were placed in the beam of the 3-MeV Van de Graaff (horizontal) accelerator of the EPFL. The pulse length was 500 ns. A 450-W high-pressure Xe arc lamp and a 320-nm cutoff filter were employed for illumination, and the monochromated light was detected with a Hamamatsu photomultiplier (PM) operated at 700–800 V. By means of a shutter system the sample was exposed to the arc light only a few seconds before and after the pulse to avoid heating and photolysis. Provision was made for magnetic stirring in cases where the decay of neutral **1** was slow in order to establish homogeneous conditions in the sample prior to each pulse. The output from the PM was sampled by a Tektronix digital storage oscilloscope and transferred to an HP 85 calculator to perform automatic first- and second-order analysis of the trace. The upper limit for the time scale of the experiment, determined by lamp instabilities and diffusive broadening of the beam volume, is on the order of 1 s, which confines the observation

† Technical University of Aachem.
‡ Ecole Polytechnique Fédérale de Lausanne.

(1) See: Kemmit, W. R.; Russell, D. R. In *Comprehensive Organometallic Chemistry*; Stone, F. G. A., Abel, W. E., Eds.; Academic: Oxford, England, 1982; Vol. 5, p 246 ff.
(2) See: Sheets, J. E. *J. Organomet. Chem.* **1979**, 64.
(3) (a) Miyake, A.; Kondo, H.; Aoyama, M. *Angew. Chem., Int. Ed. Engl.* **1969**, *8*, 520. (b) van Akker, M.; Jellinek, F. *Recl. Trav. Chim. Pays-Bas* **1971**, *90*, 1101.
(4) Salzer, A., University of Zürich, private communication.
(5) A mixture of fluorinated sulfonic acids, $C_nF_{2n+1}SO_3H$, with n ranging from 4 to 8 was kindly supplied by Hoechst AG, Frankfurt/Main, FRG.
(6) 2-Propanol was found superior to formic acid or Zn^{2+} as a quencher of $OH^\bullet$ in the acidic medium.

0020-1669/88/1327-0879$01.50/0 © 1988 American Chemical Society